Experienced-induced immediate early gene expression in hippocampus after granule cell loss

James Cardiff
B.Sc. Neuroscience University of Lethbridge, 2010

A Thesis
Submitted to the School of Graduate Studies
of the University of Lethbridge
in Partial Fulfillment of the
Requirements for the Degree

Masters of Neuroscience

Department of Neuroscience
University of Lethbridge
LETHBRIDGE, ALBERTA, CANADA

© James W, Cardiff. 2012

Abstract

Adrenalectomy (ADX) has been shown to cause selective degeneration of granule cells in the dentate gyrus (DG). This occurs due to the reduction of corticosterone (CORT) and behavioural deficits are associated with the loss of these neurons. Dentate lesions and cell loss associated with ADX have been shown to effect behaviour in a number of spatial tasks. In contras, it has been shown granule cell loss does not affect the specificity of place cells in CA3 and CA1. We used the ADX model to examine the role of DG granule cells plays in representing space using immediate early gene (IEG) activation in the principal hippocampal subfields after exploration of novel environments. Rats were allowed to free explore multiple novel environments and then the mRNA for the IEG Homer 1a (H1a) was used as a marker of neural activity. After degeneration of approximately half of the DG granule cells we found a significant increase in number of active cells in the DG, CA3 and CA1 in ADX animals. The results indicate a reduction in granule cells causes a dramatic increase in the proportion of remaining DG granule cells in response to exploration. The change in DG activation disrupts the representations in CA3 and CA1 and thereby affects behaviour.

Acknowledgements

First I would like to thank Dr. Robert Sutherland. His knowledge, experience and guidance has been invaluable during my Masters and was always able to provide useful insight and advice when need. I would also like to thank all the past and present members of the Sutherland lab for their help, support and making the lab a fun and enjoyable place to be. Specifically, Melinda Wang for always willing to lend a hand no matter what and being really good at the things I'm not so good at.

I would like to thank the McNaughton lab, especially Valarie Lapointe for helping me with the IEG protocol. Thanks must also go out to Dr. Artur Luczak and Vivek Trivedi for teaching me how to program and helping me develop the programs used in my thesis. I would also like to recognize my Masters committee members, Dr. Robert McDonald, Dr. Bruce McNaughton, and Dr. Igor Kovalchuk.

Finally I would like to thank my family, friends and fellow graduate students for being supportive and helpful over the last two years. Without all of them my Masters would not have been as enjoyable or productive, I cannot thank you enough.

List of Figures **Page**

Figure 1: Representation of trisynaptic pathway 5
Figure 2: Confocal photographs of control and ADX dentate gyrus 20
Figure 3: Scatter plot of number of neurons found in DG 21
Figure 4: Mean neuron number 22
Figure 5: CORT level 23
Figure 6: Mean H1a expression in DG 24
Figure 7: Mean H1a expression in CA3 25
Figure 8: Mean H1a expression in CA1 26
Figure 9: Percent of H1a expressing neurons in DG 27
Figure 10: Scatter plot of Number of Neurons vs Percent of H1a neurons 28
Figure 11: Scatter plot of percent of H1a neurons vs H1a expression in CA3 28
Figure 12: Mean H1a expression in all hippocampal sub field for 1 vs 5 environments 48

List of Abbreviations

ADX = Adrenalectomy
AMPA = 2 – amino-3-(3-hydroxy-5-methyl-isoxazol-4-yl)propanoic acid)
ANOVA = Analysis of variance
BRDU = Bromodeoxyuridine
CCAC = Canadian Council on Animal Care
CORT = Corticosterone
DAPI = 4', 6-diamidino-2-phenylindole
DEPC = Diethylpyrocarbonate
ETC = Electro Transcriptional Coupling
FISH = Fluorescence In situ Hybridization
H1a = Homer 1a
IEG = Immediate early gene
NMDA = N-methyl-D-asparate
PBS = Phosphate buffered saline
PFA = Para formaldehyde
RNA = Ribonucleic acid
SSC = Saline-sodium citrate
TBS = Tris-buffered saline
TBST = Tris-buffered saline with Polysorbate 20
UTR = Untranslated region

Table of Contents

Title Page	i
Approval/ Signature Page	ii
Abstract	iii
Acknowledgements	iv
List of figures	v
List of abbreviations	vi
Table of Contents	vii
Introduction	**1**
Hippocampus and Memory	2
Dentate Gyrus	4
Adrenalectomy	6
Immediate early genes	7
1 vs Multiple environments	9
Hypothesis and Experimental Goals	10
Methods	**12**
Animals Used	12
Adrenalectomy Surgery	12
CORT level analysis	13
CORT replacement	14
Experimental Exposure procedure	14
Perfusion	15
Hippocampus removal	15
Fluorescence In situ Hybridization (FISH) Labeling	16
NeuN Labeling Procedure	18
Number of Neurons and H1a Counting Procedure	18
Statistics	19
Results	**19**
Number of Neurons	19
Blood CORT Levels	22
Number of Homer 1a Positive Cells	23
Discussion	**29**
References	**44**
Appendix 1	**47**
One vs Five Environments	47
Appendix 2	**48**
Automated H1a counting program	48
Stereology estimate program	55
Appendix 3	**60**
H1a Probe Sequence	60

Introduction

Memory is the "ability to recall or recognize previous experience" (Kolb and Whishaw, 2009). It is a concept any person can understand but has proven difficult to determine in detail exactly how it works. Experimentation on memory has created as many questions as answers and shown that there is still much to be discovered about the biological mechanism of memory. Discoveries on how memory works will have numerous applications to human life. They could help people suffering from memory deficits due to disease or trauma such as Alzheimer's and traumatic brain injury through prevention and treatment. One in ten people in Canada (Alzheimer's Society of Canada) will have Alzheimer's disease and will require time and effort from their family and professional help to maintain a good standard of living. Traumatic brain occurs in thousands of Canadians each year (The brain injury association of Canada) and the individual and their families must live the rest of their life with this deficit. Any information on how the brain works will help find solutions or prevent debilitating deficits will have profound effect on the people and families dealing with brain trauma. Finally it will help us to understand human behaviour and how the brain works. For example we know that there are multiple memory systems and different parts of the brain are responsible for each types but we don't know how many different memory systems there are in total, where they are located or how they all work together to create the human experience.

This thesis examines the effects of degeneration of a set of neurons in the hippocampus, a key structure in the formation of long-term memories. We use a cellular marker for neural activation that permits visualization of the representation after rats explore new environments at the level of single neurons distributed throughout the hippocampus. The intention is to measure changes in the way new environments are represented in hippocampal neural circuitry after slow degeneration of the majority of neurons in a principal subfield of the hippocampus and thereby gain information about the nature of information representation and potentially how the loss of neurons causes memory problems.

Hippocampus and Memory

The hippocampus is thought to play a role in memory for a long period of time but it was Scoville and Milner (1957) that provided compelling empirical evidence the hippocampus plays an important role in human memory with their patient HM. HM suffered from epilepsy as a result of a childhood closed head injury. He received surgical bilateral removal of medial temporal lobe to reduce the seizures that began after the injury. The surgery was successful but left him with severe retrograde and anterograde memory deficits. HM could no longer create new explicit memories such as learning a new fact or a set of numbers. He still had intact implicit memory, which is involved in supporting performance in tasks like mirror tracing task. For this task the patient has to trace a pattern while looking at their hand reflected

through a mirror, HM was able to perform well in this task, and learned at the same rate as any person with an intact brain. The discoveries on HM's amnesia triggered an escalating programme of research on the role of hippocampus in memory, which continues to this day.

The hippocampus has been found to play a role in many different abilities, spatial navigation (Morris et al., 1982; Sutherland et al., 1982), context memory (Sutherland and McDonald, 1990), and path integration (Mittelstaedt and Mittelstaedt, 1980; McNaughton et al., 2006). Although there is controversy in the literature about whether memories remain indefinitely dependent on the hippocampus (Sutherland et al., 2008; Kim and Fanselow, 1992) it is fairly well known that the hippocampus is involved in forming stable context representation composed of spatially selective place cells (Muller, 1996).

The principal cells in the dentate gyrus (DG) are granule cells and pyramidal cells in the *cornu ammonis* (CA) regions. Granule cells are very small and tightly packed cells while the pyramidal cells are the typical neuron with triangular soma and apical/basal dendrites. Both types of principal cells in freely moving animals have firing characteristics of firing bursts of action potentials in specific locations of an environment. These are termed place cells (O'Keefe and Dostovsky, 1971). Place cells are thought to be responsible for memory of a space and communicate the information with the rest of the brain. Place cells will remap when placed in a new context and their rate of firing changes with changes of features in the environment

(Muller and Kubie, 1987; Muller, 1996). When placed in a new environment every cell has a probability that it will represent an area and fire in a specific location with no obvious relation to previous environments. If minor changes are made to the environment the cells use a different strategy called rate remapping (Leutgeb et al., 2005). This is when the cells keep the same firing fields but change their firing rate, signaling a change in the environmental representation. This same phenomenon occurs when new objects are introduced to an environment, but apparently only to the cells surrounding the perceived change (Muller and Kubie, 1987).

Dentate Gyrus

The DG is a subfield of the hippocampus. The principal cells are called granule cells and they receive a strong input from layer 2 of the entorhinal cortex. The entorhinal-dentate axons form the perforant pathway and the axons connect to the molecular layer of the DG where the granule cells dendrites are found. The axons from the granule cells project to CA3 (fig. 1) and are called mossy fibers (Amaral and Witter, 1989) and mainly interact with interneurons but some connect with the pyramidal cells of CA3 as well.

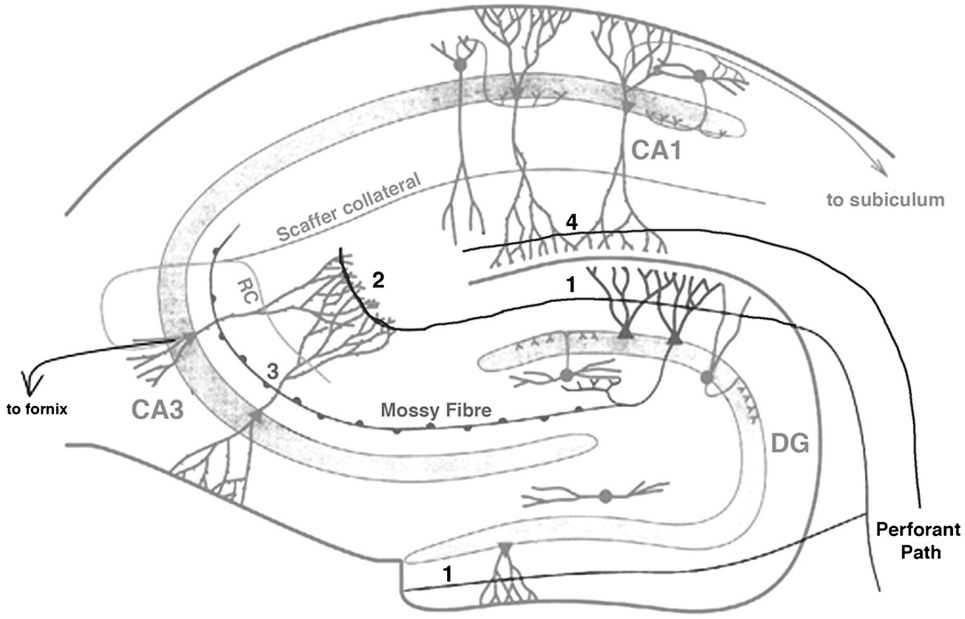

Figure 1: Representation of connections and flow of information in the trisynaptic pathway in the hippocampus (Daumas et al., 2009)

Lesion studies have revealed damage to the DG produces behavioural deficits in spatial tasks such as Morris water task (Sutherland et al., 1982; Xavier et al., 1999) and radial arm maze (Vaher et al., 1994). Electrophysiological studies of CA1 and CA3 after dentate lesion found there is little or no effect on spatial specificity of the place cells. They did find that there was reduction in reliability of spatial firing from trial to trial (McNaughton et al., 1989).

Current theories posit granule cells in the DG are responsible for pattern separation, reducing interference from similar contexts by representing them with different firing patterns. As information flows through the hippocampus (DG-CA3-CA1) it is believed the pattern of activation becomes more distinct for each experience. If this

is true then the dentate, being the first structure, would be responsible for the original separation of similar stimuli. The granule cells in the cerebellum have a similar physiology and provide a similar role of pattern separation for input to cortical structures (Chadderton et al., 2004) and it is believed that the granule cells of dentate play a similar role for the rest of the hippocampus. Computational models of memory have also suggested the dentate is responsible for separating similar stimuli and relaying it onto CA3 to help create distinct representations (Treves and Rolls, 1992). Behaviour data from DG lesion and adrenalectomy support this theory as well; deficits in object context association and spatial memory (Spanswick et al., 2010; Sutherland et al., 1982).

Adrenalectomy

Adrenalectomy (ADX), bilateral removal of the adrenal glands, was first discovered to selectively reduce the number of granule cells in the DG by Sloviter et al. in 1989. The neuron loss is caused by a reduction of circulating corticosterone (CORT) and only effects the granule cells in the dentate gyrus (Sousa et al., 1997). Sloviter et al. also showed cell death could be prevented by chronic intake of CORT and all other cells in the hippocampus stay healthy and functional despite loss of granule cells.

CORT prevents cell death by activating the type 1 adrenal steroid hormone receptor; other agonists of this receptor also prevent cell death (Woolley, 1991). When the

granule cells lack activation of this receptor it increases the number of pyknosis cells present in the dentate (Gould, 1990), which is the beginning of apoptosis. Cell death begins less than 2 days after surgery and increases until reaching a plateau around 4 weeks and then declines up to 23 weeks (Jaarsma et al., 1992; Spanswick et al., 2011).

The cause of behavioural deficits after ADX has been a controversial topic. Initially it was reported there was a deficit in initial learning in the Morris water task and a deficit in responding to cues changing (Armstrong et al., 1993). Later it was discovered the deficit in learning the Morris water task could be at least partially reversed with short term CORT replacement (McCormick et al., 1997; Spanswick et al., 2007). In contrast, recently it has been shown that even with short term CORT replacement a deficit is still seen in more difficult tasks such as object-context mismatch (Spanswick et al., 2010). The loss of granule cells effects behaviour in difficult situations involving specific details. The effect found in granule cell loss from ADX is not fully congruent with the granule cell loss from lesion studies mentioned previously but the difference is likely attributed to ADX causing loss of only half of the granule cells, while lesions destroy a larger proportion of the cells in the dentate.

Immediate Early Genes

Immediate early genes (IEG) are genes that undergo transcription and translation shortly after a neuron has been activated to a sufficient degree. The RNA transcripts can be labeled and thus a marker of neuron activity can be quantified after the fact (Lanhan and Woorley, 1998).

In 1997 Brakeman et al. discovered Homer 1a (H1a), a 6.5 kb long gene encoding a protein of 189 amino acids that was responsive to synaptic activity. It is brain specific, highly up regulated in the hippocampus and production of RNA begins around 30 min and continues up to 4 hours. The H1a protein is found at synapses enriched in GluR1 receptors and is found to bind to them and play a role in synaptogenesis and receptor trafficking (Xiao et al., 2000). Specifically the H1a protein increases AMPA receptor expression and synaptic signaling without affecting the NMDA receptor (Hennou et al., 2003). H1a has successfully been shown to be an effective IEG in the hippocampus and can begin to be labeled ~20 min after exposure and start decreasing around ~40 min (Vazdarjanova et al., 2002).

Electro transcriptional coupling (ETC) is the term for the association between neural activity and production of IEG mRNA (Guzowski et al., 2006). Guzowski et al. (2006) completed an interesting study displaying the plasticity of ETC on the IEG Arc. They looked at the effect of previous experience on a cell's ability to express and be successfully labeled for Arc. They discovered recent exposure to previous environments lowered the ability to for cells to express Arc mRNA after exposure to the same environment previously experienced but not to a novel environment. This

shows that the mechanisms responsible for transducing action potentials into gene transcription are can be altered and is sensitive to previous experience.

1 vs. Multiple Environments

To study how the hippocampus encodes different environments a recent paradigm has been used of exposing an animal to either 1 or multiple unique environments and looking at IEG expression. The idea behind this theory is a set of place cells become active during each exposure to an environment and exposure to multiple environments increase in the number of IEG positive cells due to multiple maps being recruited. Some cells will be present in multiple maps so the increase in the IEG signal should not be linear. A look at the current literature using IEG and multiple environments brings up many questions.

Vazdarjanova and Guzowski (2002) used 2 IEGs (ARC and H1a) with different time courses synchronized with specific context to see the overlap between the two contexts in CA1/3. They found approximately 15% of the cells were active in CA3 and 35% of cells active in CA1 for either environment. But only 2% of cells were active in both contexts. Chawla et al. (2005) described an experiment placing a rat in either 1 or 2 unique environments then used ARC to label active cells in the DG. They found an increase in activation when exposed to more than one environment

and approximately 0.1% of cells were active in one environment and 0.6% were active when exposed to both environments. Alme et al. 2010 preformed a similar experiment with 4 environments and looked at DG as well. They found an increase when exposed to multiple environments but to a lesser extent. % were active in 4 environments and 1.5% active in 1 environment.

The literature does not give an unambiguous answer to how the hippocampus activity is affected by exposure to multiple environments. The change from multiple environmental exposures in dentate is from 30% - 600% increase and a proportion active from 0.1% to 4%. The exact cause of ambiguity is unknown but is likely due to the counting techniques and other experimental procedure. Some of the counting techniques used have involved exhaustive counting of very small proportion of the total area. This can lead to bias results because the the whole structure is not equally sampled. Experimental procedures have varied among studies and involved confounding details such as objects present in environments, open field environments, and experimenter-assisted exploration.

Hypothesis and Experimental Goals

The goal of this project was to further characterize the neurocognitive effects of hippocampal granule cell degeneration caused by ADX. Specifically, we sought to understand how DG degeneration changes the activity pattern of the remaining

neurons in the DG and downstream regions of the hippocampus (CA3, and CA1) after exploration of novel environments. Since it is established that a significant proportion of the behavioural effects of ADX is caused by loss of granule cells (Spanswick et al., 2010), knowing how the activity of neurons in the DG and downstream areas is altered will lead a deeper understanding of how this neuron loss might lead to memory problems. This information will also provide insight into the role DG plays in the hippocampus, specifically if granule cell loss significantly alters the degree of activity overlap in different explored environments.

For this study it was planned to have four independent groups of rats, control and exposure to one or five novel environments, ADX and exposure to one or five novel environments. The adrenal glands of rats were bilaterally removed causing the DG to degenerate over eleven weeks due to low level of circulating CORT. During the last week (week 12) CORT was replaced in adrenalectomized rats to ensure any change detected is due to changes in cell number not CORT levels. Control and ADX rats were exposed to either one or five novel environments followed by labeling for IEG H1a and analysis of number of H1a positive cells in DG, CA3, and CA1.

I predicted in ADX rats the overlap in neurons activated in one vs. multiple environments would be increased (consistent with reduced pattern separation). Evidence for pattern separation across multiple environments has been seen in experiments performed by other researchers (Leutgeb et al., 2005). This prediction is based on the fact rats with ADX display behavioural deficits in object/context

associations, Morris water task and radial arm maze. Unfortunately no difference between one and multiple environments was found in control animals so this hypothesis could not be tested. I also anticipated both ADX groups (one and multiple environments) would shown similar or lower cell activity to controls exposed to one environment. But interesting the prediction was incorrect and we saw the complete opposite effect.

Methods

Animals Used

23 male Long-Evans rats were obtained through Charles River and experimentation began after the rats were approximately 75 days old. They were caged in pairs with a 12 hour light-dark cycle (on at 7:30) and *ad libitum* access to food and water for duration of the study. The University of Lethbridge and Canadian Council on Animal Care (CCAC) approved all procedures.

Adrenalectomy Surgery

13 rats underwent ADX and 10 control surgery. Half an hour before surgery began rats were injected with buprenorphine (0.05 mg/kg, i.p.) to reduce pain. A slow

increase from 1% to 4% concentration of isoflurane (1.5 liters of oxygen per minute) was used for induction and 2% for remainder of surgical procedure. During induction flanks were shaved and sterilized using alternating swabs of Hibitane® (4% chlorhexidine gluconate) then alcohol (70% isopropyl) repeated 3 times. ADX began with a 4 cm incision through the skin beginning just below ribs using a number 11 scalpel. The initial muscle incision was made with the scalpel as well but was increased in size by stretching and causing natural tearing of the muscle. The adrenal glad was removed using organ forceps and then the muscle and skin was sutured closed (Vicryl 3-0 coated, Ethicon Inc.). Control surgeries were preformed the same but no incision was made through the muscle or adrenal gland removed to help prevent infection. Immediately after surgery and 12 - 24 hours later rats were injected with Metacam (0.1mg/kg) to help with pain and any possible infection. All ADX rats were given 0.9% saline in lieu of normal tap water.

CORT level analysis

8 weeks after surgery rats were anesthetized (same as surgery), the tail was swabbed with alcohol and approximately 1.0 ml of blood was collected using a Heparin (Sandoz Canada Inc.) coated 23-gauge needle from a tail vein. Blood samples remained on ice until they were centrifuged at 8,000 rpm for 10 minutes. Serum was drawn off and kept at -80 °C until samples were assayed. Analysis of samples was completed using AB Chem Elisa kit.

CORT replacement

11 weeks after ADX animals were given CORT replacement (1mg per rat per day). CORT was dissolved (4mg/ml) in sesame seed oil and 0.25ml was placed on Dad's peanut butter oatmeal cookie and given to rats once a day at 16:00 (Spanswick et al. 2007). Control rats were given the same but without the CORT dissolved in the sesame seed oil.

Experimental Exposure Procedure

12 weeks after ADX or control surgery and one week after CORT replacement began rats were exposed to either 1 (5 control and 6 ADX) or 5 (5 control and 7 ADX) novel environments. The environments were located in different rooms and rats were transported in a normal clear carrying cage with corncob bedding. All environments varied somewhat in size (2m^2 +/- 0.75m^2), shape and construction material. Rats were allowed to freely explore the environment for 2 min and were then placed back in the carrying cage and moved to a new environment or placed back in the previous environment after 1 min allowed for travel. They were then placed back in home cage for 25 min before perfusion.

Perfusion

All perfusion equipment was cleaned using RNAse away to prevent contamination for in situ labeling. Rats were injected with a lethal dose of sodium pentobarbital (500 mg/kg, i.p.) and perfused transcardially with approximately 200 ml of phosphate buffered saline (0.1M PBS) followed by an equal volume of a 4% paraformaldehyde (PFA) solution. Brains were extracted and stored in the same 4% PFA solution (24 hours for right hemisphere, 3 hours for left) and then transferred to sucrose.

Hippocampus removal

All equipment used in handling the brains was cleaned using RNAse away to prevent contamination for *in situ* labeling. 3 hours after submersion in PFA left and right hemispheres were separated and the right hemisphere was placed back in PFA for the remainder of 24 hours. Hippocampi were removed from the left hemisphere and placed in sucrose. For removal of hippocampus first brainstem and midbrain were slowly teased back and removed exposing the hippocampus. Then beginning at the fornix and moving to the entorhinal cortex the hippocampus was slowly pealed back and removed. The entorhinal cortex was then cut to free the hippocampus from the rest of the cortex. The hippocampus was placed in sucrose.

After 24 hours in sucrose the hippocampi were blocked and sectioned. 10 – 14 hippocampi per block were punctured using insect needles and placed vertically in a plastic mould (2 moulds were used for this experiment). Moulds were then filled with Tissue Tec and frozen at -20C and stored at -80C until sectioning. Blocks were sectioned using cryostat and mounted on Fisher Brand Superfrost Plus slides and stored at -80C for *in situ* labeling.

Fluorescence In situ Hybridization (FISH) Labeling

H1a antisense riboprobe was generated using an H1a cDNA clone and was directed to the 4.4 kb 3'untranslated region (UTR) of the H1a mRNA (Brakeman et al., 1997; Vazdarjanova et al., 2002). Briefly, riboprobe was synthesized using a commercially transcription kit (MAXIscript Kit; Ambion, Austin, TX) and fluorescein-labeled UTP (Roche Diagnostics; Indianapolis, IN). It was purified using mini Quick Spin columns (Roche Diagnostics; Indianapolis, IN) and verified by gel electrophoresis (see Appendix 4 for probe sequence).

Day 1

Slides taken out of freezer and given an hour to warm up to room temperature. Incubated in 4% PFA for 4 min on ice (approximately 4C) then washed in 2x SSC for 2 min. 30 min in TBS chamber with proteinase K then incubated in PFA for 3 min (on ice again) and washed with 2x SSC for 2 min. Then submerged in acetic

anhydride solution (NaCl, DEPC water, triethanolamine and acetic anhydride) for ten minutes then briefly dipped in DEPC water to remove any left on the slide before being submerged in 1:1 solution of -20C acetone methanol (on ice) for 5 min. Wash in 2x SSC for 5 min followed by prehybridization (cover slip) for one hour and then a probe/buffer solution over night at 56C (probe 0.7 ng/ul).

Day 2

Slides are taken out of oven for 15min to cool down to room temperature. Washed in 2x SSC for 5 min then 10 min and then RNase A and 2x SSC (10 ug/ml) at 37C for 30 min. Two 5min 2x SSC washes and one 10 min 0.5x SSC wash followed by a 30 min 55C 0.5x SSC wash and 5 min 0.5 SSC wash. Slides are then quenched in 2% H2O2 in 1xSSC for 15 min and two 5 min TBST washes. One 5 min TBS wash followed by blocking buffer with 5% sheep serum (cover slip) for 1 hour in TBS chamber and then 1:1000 anti-FL (peroxidase conjugated IgG fraction monoclonal mouse anti-fluorescence) (Jackson ImmunoResearch Labs Inc, PA) and blocking buffer overnight at 4C.

Day 3

Three 10 min TBST washes followed by 1:100 FITC FL-tyramide signal amplification kit (PerkinElmer, Boston, MA) for 30 min (cover slip) followed by another three 10 min TBST washes and one 5 min TBS wash. Finally 1:2000 DAPI and TBS for 60 min (cover slip) followed by one final TBS wash and coverslip using Vectashield. Stored in the dark at 4C.

NeuN Labeling Procedure

Right hemispheres were cut at 40 um on a microtome and stored in 2% sodium acetate in PBS. Slices were washed in PBS then placed in primary antibody NeuN (Chemicon International, Temecula CA) 1:2000 + 0.3% triton x for 24 hours. Three 7 minute PBS washes before secondary labeling of Alexa Fluor 488 donkey anti-mouse IgG (Molecular probes, Carlsbad CA) at 1:500 for 24 hour, DAPI was added for the last half an hour followed by three final PBS washes. Sections were then mounted on 4% gelatin slides.

Number of Neurons and H1a Counting procedure

NeuN-positive cells were counted using the optical fractionator technique from Microbrightfield's stereology software on a Zeiss fluorescent microscope. The optical fractionator technique allows unbiased cell estimates by using uniform random sampling to allow sampling from all areas in a structure. After collection of sampling sights it calculates the estimated number of cells using number of cells counted (Q), section sampling fraction (ssf), area sampling fraction (asf) and height sampling fraction (hsf) and this equation $N = \Sigma Q \times (1/ssf) \times (1/asf) \times (1/hsf)$.

H1a was counted using custom-made automated counting software. Multi layer Nanozoomer images were taken the middle layer was used and analyzed for total H1a signal. Number of slides counted varied from 10 – 16 and slides with damage to the hippocampus were excluded. See Appendix 2 for more detail.

Statistics

Statistically significant effects in NeuN, CORT and H1a were detected using a one way ANOVA with a Tukey Post Hoc test. For correlations a two-tailed bivariate analysis was used and significance was set at $p < 0.05$ for all analyses.

Results

Number of Neurons

Cell estimates using NeuN as a marker for neurons showed ADX was successful in 6 out of 13 rats and significantly reduced granule cell number (fig 2).

A

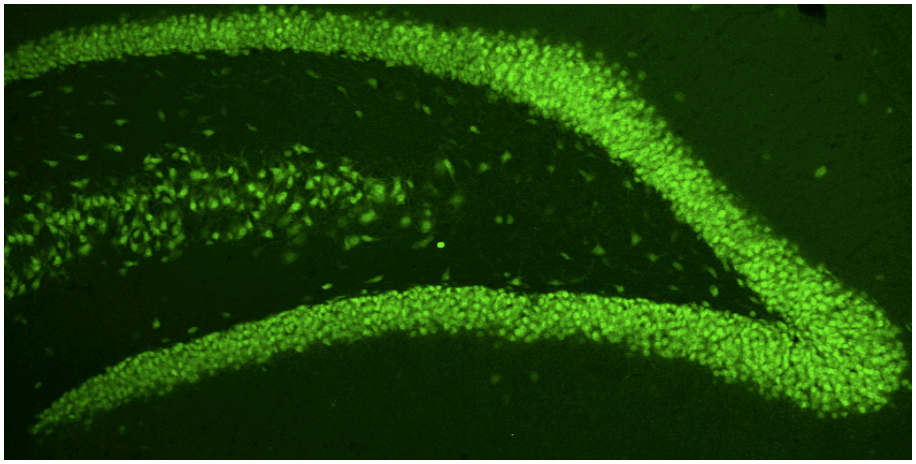

B

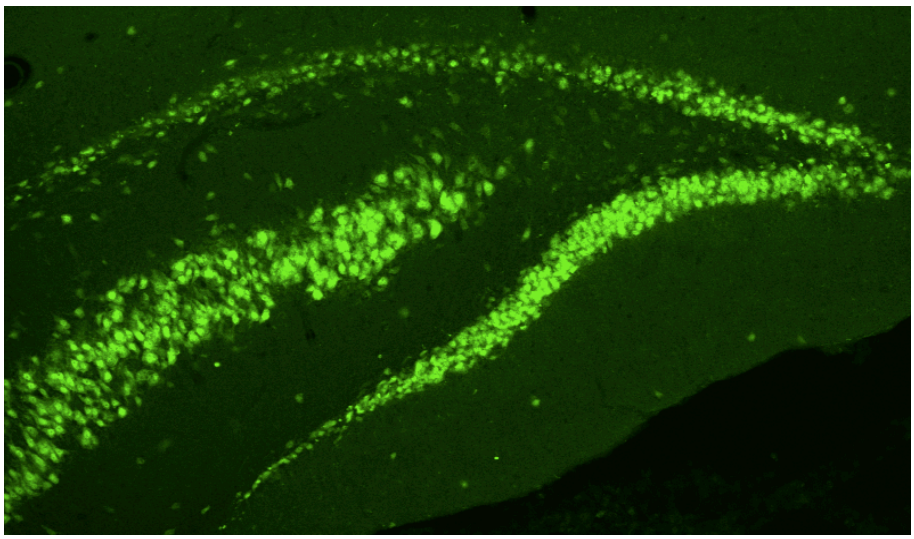

Figure 2: Confocal images of NeuN labeled neurons in DG in dorsal hippocampus of control (A) and successful ADX (B). ADX dramatically reduces number of neurons in the granule layer of the dentate gyrus. The dorsal blade of the dentate gyrus also shows greater amounts of degeneration (Intensity of image B was increased to more clearly show the few cells that remain in DG).

The reason for lack of degeneration in some cases is unknown but we divided ADX into two groups based on amount of degeneration. There was a large gap in the amount of degeneration seen in the ADX group (fig. 3) and this is the line between complete and incomplete ADX.

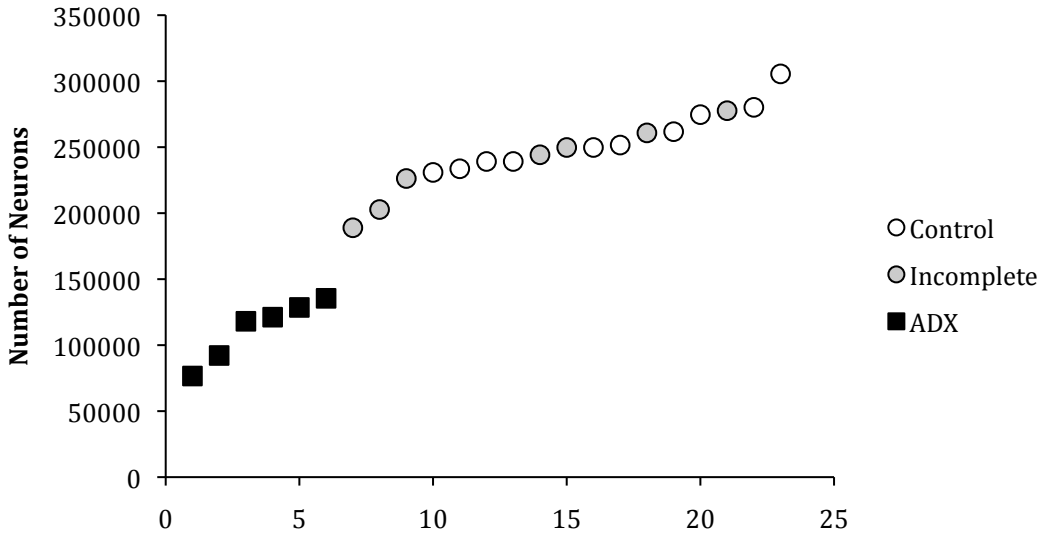

Figure 3: Estimated number of neurons in the granule layer of the DG sorted from least to greatest. The groups were distinguished by discontinuity between 140000 and 180000 cells. This discontinuity was used to determine incomplete and successful ADX and final numbers were six ADX, 7 incomplete, and 10 control.

Mean number of estimated neurons for control, incomplete and ADX was 256619.53 ± 7579.33, 235765.04 ± 11973.70, and 112012.80 ± 9297.08 respectively (fig 4). We found a significant difference between ADX and control or incomplete groups ($p < 0.001$) and no difference between control and incomplete groups.

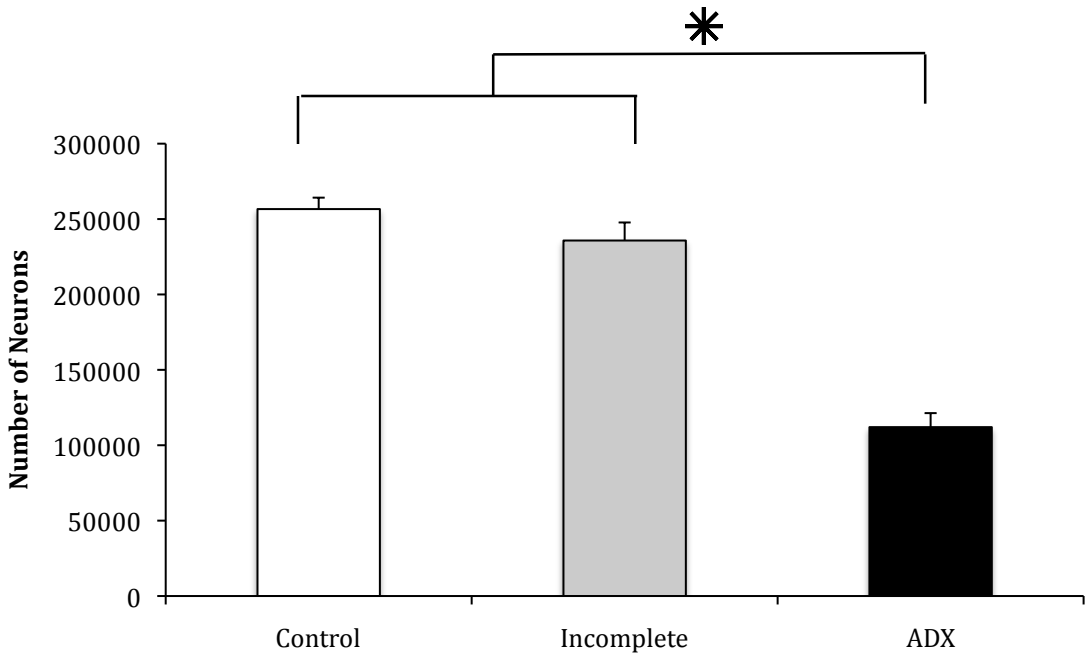

Figure 4: Mean NeuN labeled neurons in granule layer of DG. ADX group has significant decrease in the number DG neurons ($p < 0.001$). Incomplete showed no difference in number of cells from controls.

Blood CORT Levels

CORT levels were successfully reduced in all ADX animals. Controls had 404.58 ng/ml ± 79.38 of circulating CORT, incomplete had 32.67 ± 2.85 ng/ml and ADX had 31.72 ± 17.81 ng/ml. A significant difference between control and either incomplete and ADX ($p<0.005$) was found.

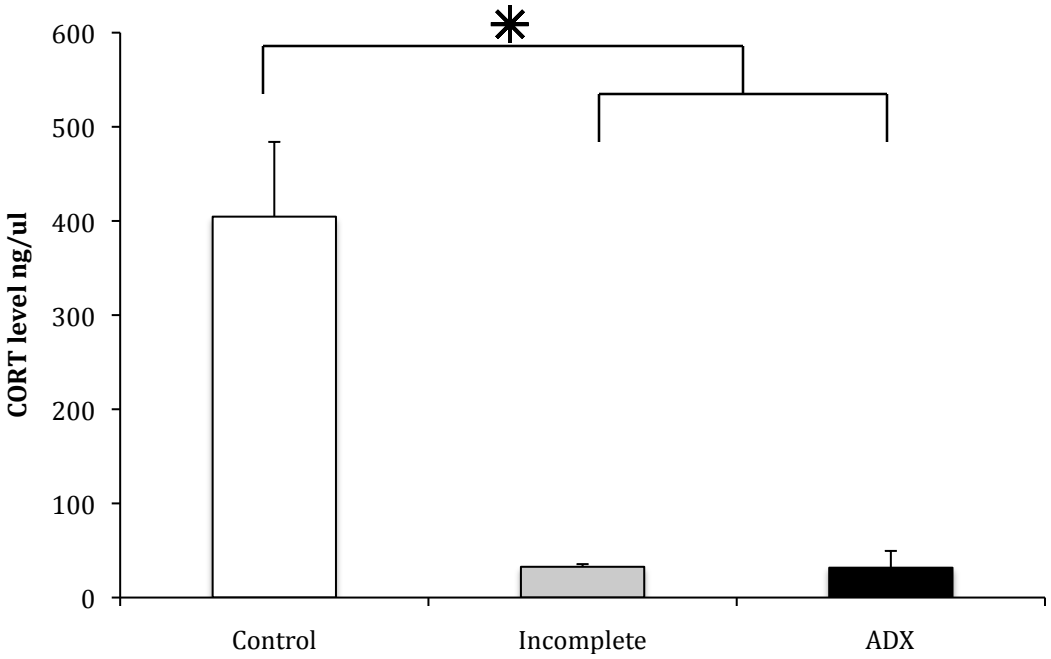

Figure 5: ADX significantly reduced CORT levels in all animals that underwent ADX. A subset of animals (incomplete) showed reduced CORT but did not have granule cell degeneration. This shows CORT level could not distinguish between successful and unsuccessful ADX ($p < 0.005$).

Number of Homer 1a Positive Cells

One vs five environments was not and important factor in this experiment and therefore is not included here, see Appendix 1. H1a signal was analyzed in DG, CA3 and CA1. In DG mean number of H1a foci per slide was calculated and control had on average 0.853 ± 0.198 foci, incompletes had 1.894 ± 0.358 foci, and ADX had 2.261 ± 0.310 foci. There was a significant difference between controls and both incomplete ($p < 0.05$) and ADX ($p < 0.005$) (fig. 6).

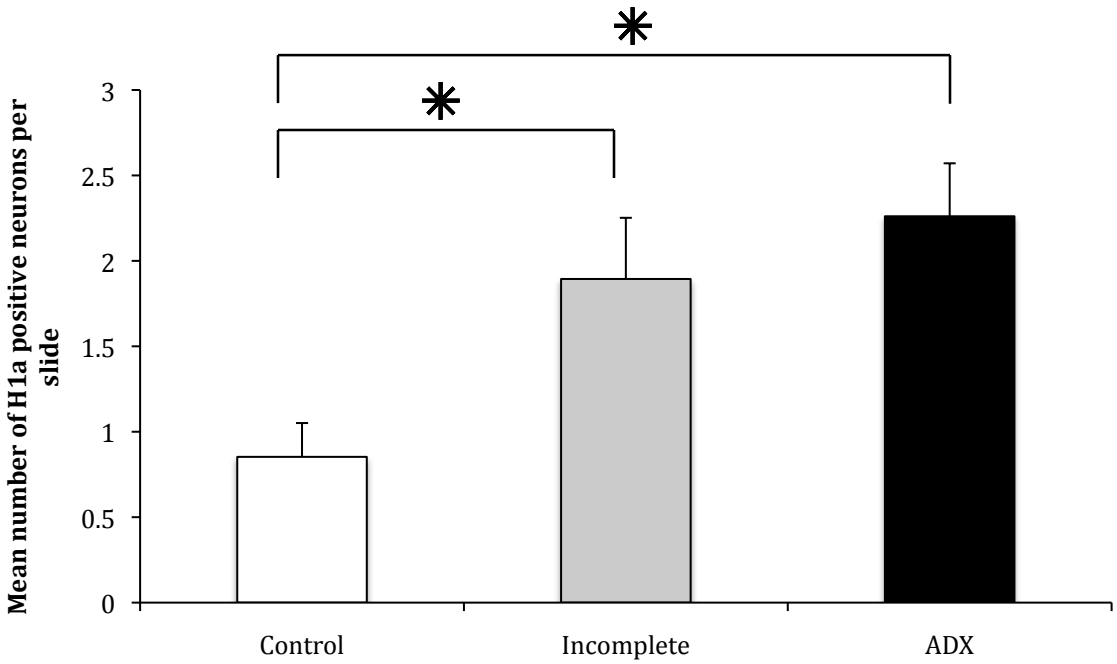

Figure 6: Mean number of H1a positive neurons in DG. Both incomplete and ADX groups had significant increase in H1a neurons compared to controls ($p < 0.05$). Does not take number of cells in the DG into account and shows a reduction of cells in the DG increase the total amount H1a positive cells present.

In CA3 average number of foci was calculated and control had 1.242 ± 0.308 foci, incomplete had 2.680 ± 0.396 foci and ADX had 3.837 ± 0.352 foci. Significance was found between Control and both incomplete ($p<0.05$) and ADX ($p<0.001$). ADX and incomplete had a p value of 0.112. As well one data point was excluded from analysis for these calculations (Rat 55 incomplete group, 17.00 foci per slide; >2 standard deviations from mean).

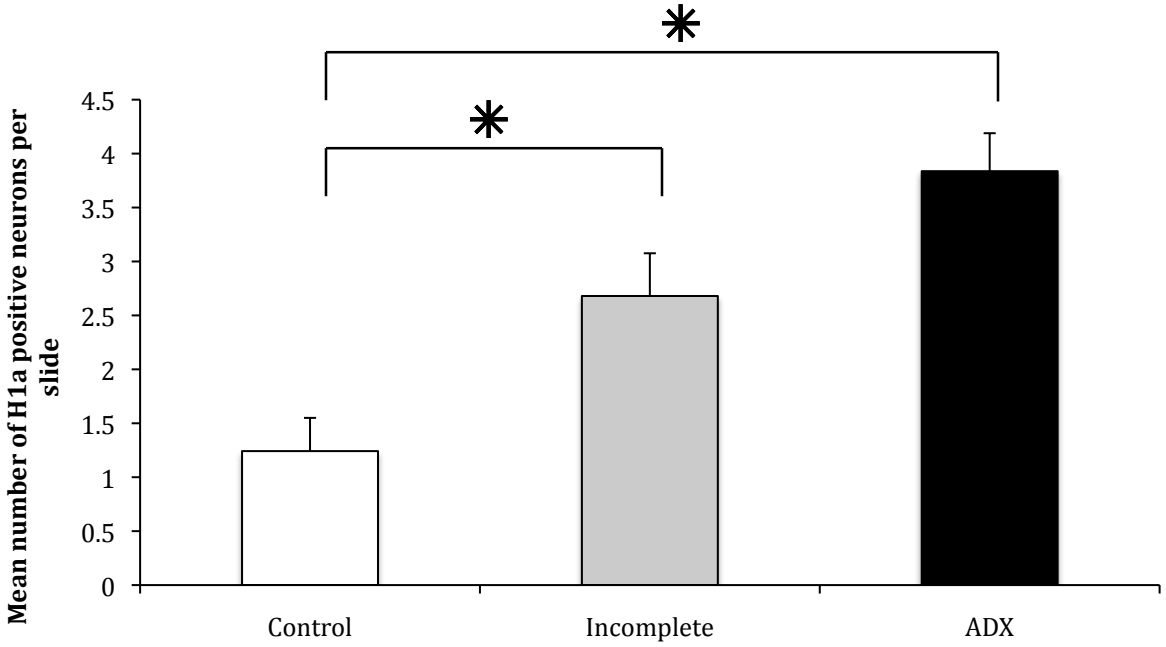

Figure 7: Mean number of H1a positive neurons in CA3 per slide in control, incomplete and ADX. Both incomplete and ADX groups had significant increase in H1a neurons compared to controls even though ADX has no effect on CA3. The increase in number of H1a positive cells must be a result of an increase in DG (fig. 6).

Same value was calculated for CA1 as CA3. Controls were found to have 2.126 ± 0.688 foci, incomplete had 2.725 ± 0.606 foci, and ADX had 6.355 ± 1.928 foci. A significant difference was found between controls and ADX groups ($p<0.05$) and one data point was excluded from this analysis (Rat 66 control group, 16.44 foci per slide; >2 standard deviations from mean).

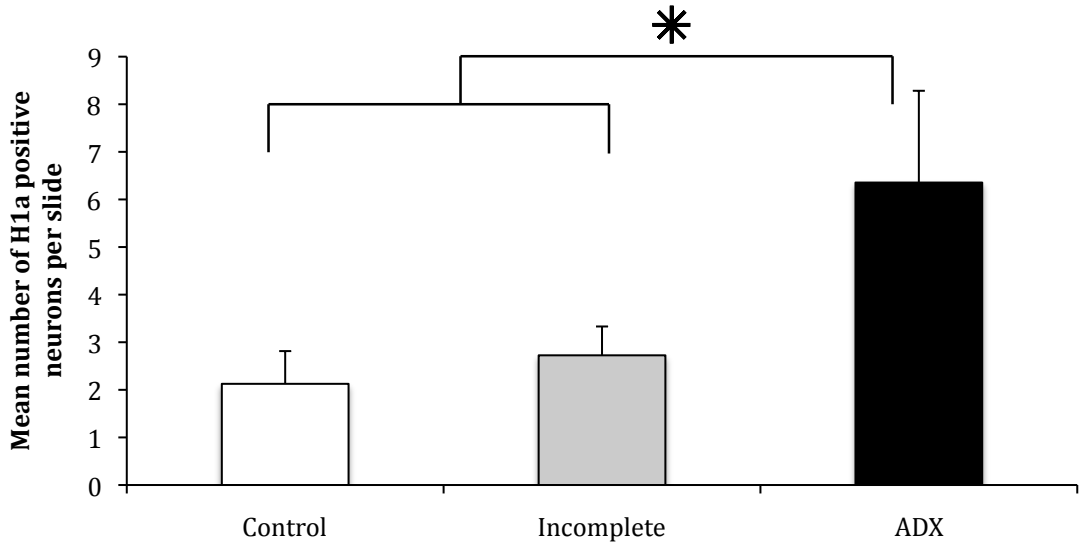

Figure 8: Mean number H1a positive neurons in CA1 per slide. ADX groups had significant increase in H1a neurons compared to controls and incomplete groups. Incomplete group also returns to control levels at this point. ADX has no effect on CA1 cells so this increase must be occurring because of the increase in DG and CA3 (fig. 6 and 7).

In DG percent active was calculated by taking the number of H1a positive neurons divided by the number of estimated neurons. Control had 0.0586 ± 0.0142 percent of cells expressing H1a, incomplete H1a expression was 0.1366 ± 0.0256, and ADX had 0.2802 ± 0.0908 percent of cells expressing H1a. There was a significant difference between ADX and both incomplete ($p < 0.005$) and control ($p < 0.001$). There was also a large difference between incomplete and control but it was not significant ($p = 0.065$).

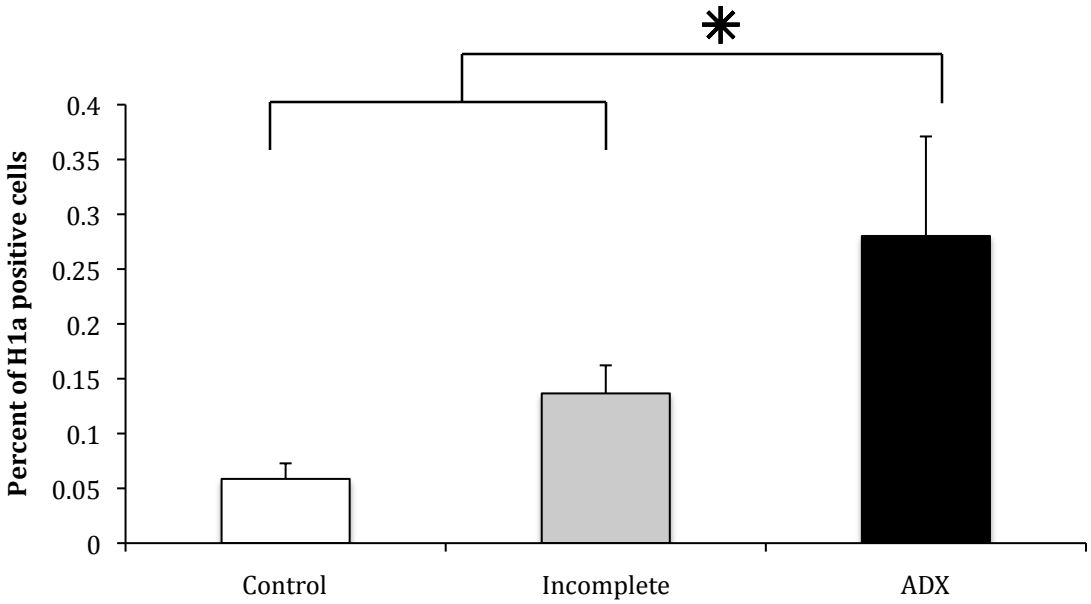

Figure 9: Percentage of H1a positive cells in DG. ADX rats display a significantly higher percent of H1a positive neurons than both incomplete ($p < 0.005$) and control ($p < 0.001$). A large but not significant difference was found between control and incomplete ($p = 0.065$). When taking number of cells into account in measurement of H1a the effect of reducing the number of cells in the DG can be seen.

Correlations were found using SPSS using all animals (2 individuals excluded from previous analysis were excluded from this as well). DG estimated number of cells and DG percent active had a significant positive correlation ($r = 0.746$, $p < 0.001$). A significant correlation was found for DG percent active and CA3 as well ($r = 0.666$, $p < 0.001$).

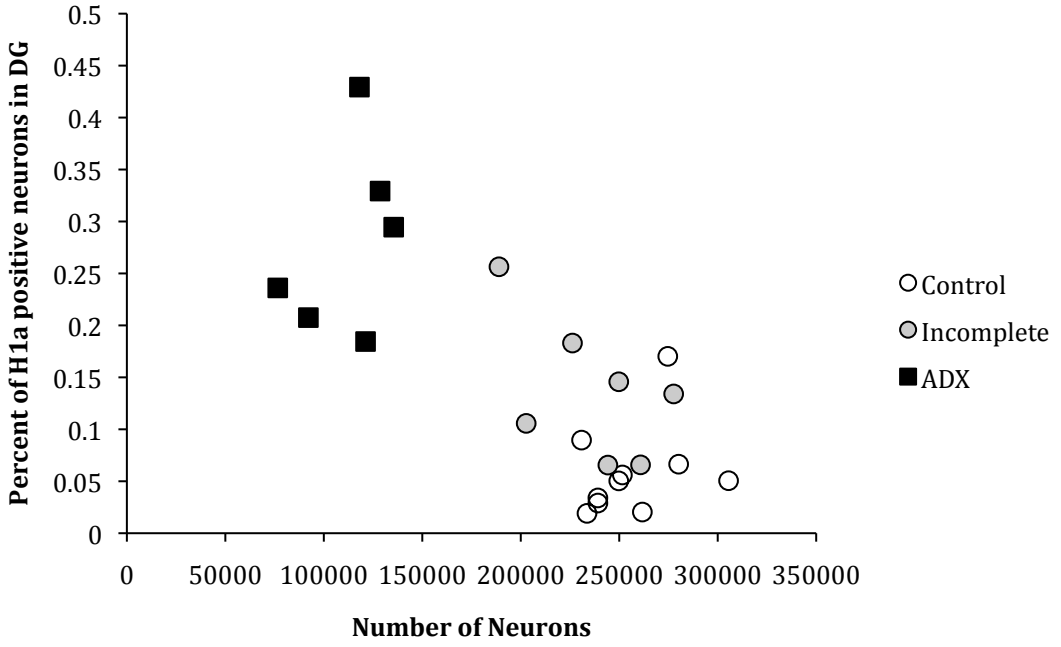

Figure 10: Scatter plot of number of neurons vs percent H1a positive in the DG. r = .0.746. Number of neurons in the DG predicts the percentage of H1a positive cells in DG.

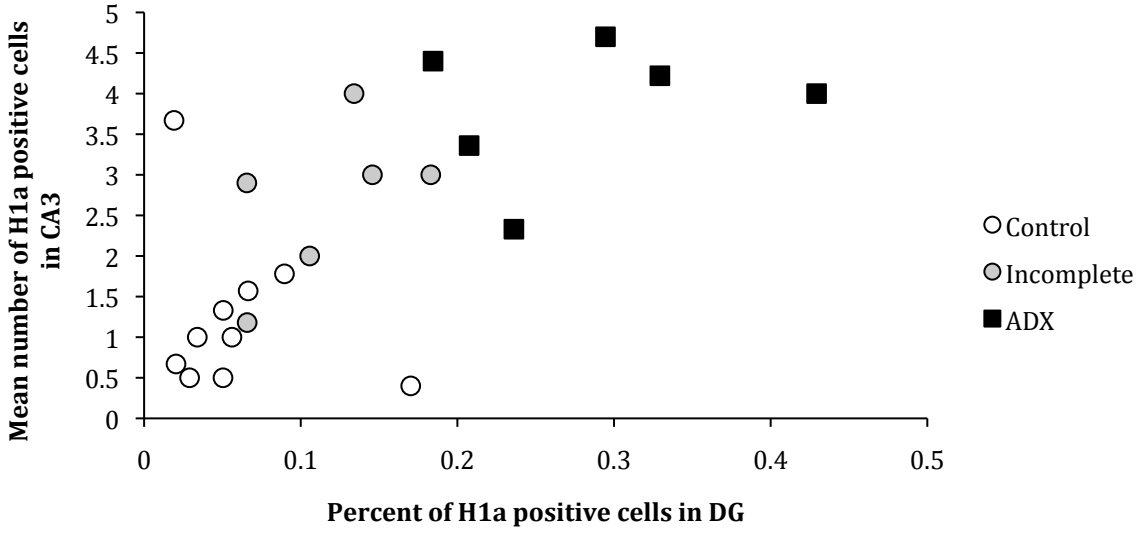

Figure 11: Scatter plot of percent H1a positive in DG and CA3 activity. r = 0.666. Percentage of H1a positive cells in DG predicts H1a positive cells in CA3, increase DG activity is responsible for increase in CA3.

Discussion

This study was performed to learn more about the role of the hippocampus, especially granule cells in the DG, in representing space. This knowledge will allow a better understanding of how the brain encodes space, memories and may provide insight into how the hippocampal information processing is changed by slow cell loss due toapoptosis in the DG (Zhongting et al., 1997). We quantified the number H1a positive cells, in DG, CA3, and CA1 after a ~50% reduction in number of granule cells in the DG caused by chronic reduction in CORT levels from ADX. In granule cell reduced animals we found a greater than 3 times increase in the number of H1a positive cells in all areas measured in the hippocampus (fig 6, 7 and 8). From this we conclude a reduction in cells causes entorhinal inputs to reorganize and increase the number of synapses on the remaining granule cells, which are younger and more excitable, causing them to increase their firing probability. This increased activation propagates through the hippocampus causing increased activation in CA3 and CA1 (fig. 11).

ADX surgeries were successful in reducing CORT levels to approximately $1/10^{th}$ of controls levels in all ADX animals (fig. 5). 46% ADX animals showed a large reduction in number of cells (fig. 4). The reason not all rats showed a dramatic loss in granule cells is unknown. This is puzzling since it has been shown activation of type 1 adrenal steroid hormone receptor prevents cell death, and this receptor is

activated by CORT. We saw no difference in the circulating level of CORT (fig.5) in ADX and incomplete animals so we parsimoniously conclude these animals had similar levels of activation of this receptor. For some unknown reason approximately half of animals did not show degeneration (fig. 3), this could be due to differences in receptor sensitivity or selectivity, individual differences in CORT levels before ADX, or some unknown protective immunity.

It is important to understand the specificity of cell death after ADX. Sousa et al. (1997) used unbiased stereology for a comprehensive study of volume and cell number in all the subfields in the hippocampus after ADX. They found no change in cell number or volume in CA3, or CA1 and found a significant decrease in DG granule cells. None of the labels for different cell types, GABA, neuropeptide Y and somatostatin, showed a change in cell number. This study provides compelling evidence for the specificity of ADX and definitively shows that ADX only affects the granule cells in the DG.

The proportion of neurons expressing H1a in the DG was significantly increased in ADX animals (fig. 9). After a 56.4% reduction in DG cell number we saw a 478% increase in the proportion of H1a positive cells in DG. This increase could be due to entorhinal inputs reorganizing to create more excitatory synapses with dendrites of the remaining granule cells. As well, ADX preferentially causes older granule cells to undergo apoptosis (Cameron and Gould, 1996) and it has been shown that very young granule cells have enhanced plasticity and more excitable membranes

(Heiber et al., 2004). The combination of increased density of excitatory inputs and increased excitability of the cells could be a basis for the dramatic increase in the proportion of H1a positive cells. Another explanation of these results would involve the strength of the H1a signal to be related to neuron firing rate which there is some evidence from unpublished data (Li, 2011). It could be ADX is causing an increase firing rate among cells in the DG, which pushes the H1a signal above the detectable threshold causing an increase number of H1a positive cells. The control cases would show few H1a positive cells because not enough H1a signal is being produced due to lower firing rate and thus can not be detected by our method. Possibly granule cell reduction causes an increase firing rate of granule cells, which boosts the H1a signal, and the signal is now detectable by our methods. This could be tested by using a lower threshold and see if IEG expression is closer to ADX levels, unfortunately the lowest threshold possible was used with the tools at our disposal and a different method would be required to tease this apart (discussed in more detail later on).

The perforant path must reorganize during loss of granule cells but how it reorganizes is not established. When half the dendrites in the molecular layer start to die off, likely the perforant path axons would start competing to make new synapses on available space on nearby surviving dendrites. This would continue until the degeneration has reached a plateau and cell death is equal to cell survival. At this point there would be more excitatory synapses on each granule cell in the ADX animals compared to controls. With approximately half the number of granule

cell dendrites available a possible case is there are twice as many excitatory synapses on each granule cell. When exposed to a novel environment the entorhinal cortex would provide the same amount of excitation through the perforant path axons but on half the granule cells with many more synapses on the remaining cells, there would be an increased probability of the remaining cells being strongly activated.

The granule cells remaining after degeneration should be, on average, younger than the granule cells found in a normal DG. Cameron and Gould (1996) used BRDU to determin the ages of granule cells at 3 time points (1, 14 and 54 days before ADX) and found 60% ADX and 40% of Control were at the 14 day injection, implying that the older granule cells had died off. It is known that these younger cells (2-6 weeks) are more easily brought to threshold for spiking, thus less excitatory synaptic drive is needed to cause an action potential (Schmidt-Hieber et al., 2004). As stated before, the combination of increasing the number of excitatory synapses per granule cell and the fact that remaining ADX neurons are younger, thus more excitable, are plausible bases for the large increase in the proportion of H1a positive granule cells after exploration of novel environments.

There was a similar increase in the proportion of H1a positive neurons found in CA3, the DG's downstream target connected via excitatory mossy fibers. This increase in CA3 is smaller in magnitude compared to the increase found in DG. In CA3 the increase was 309%, compared to 478% in the DG. The main direct extrinsic

excitatory inputs to CA3 are from mossy fibers and the projections from entorhinal cortex. Likely the increase in CA3 activation could come from the mossy fibers excitatory projections. It could be a ~50% reduction in the number of mossy fiber connections and potentially a 4-fold increase in the number of mossy fibers firing at any one time, due to the decrease in the number of granule cells and an increase in number of active cells. We found a very similar increase in CA1 activation. An increase of 299% in the number of H1a-positive neurons was measured in CA1, and, like in CA3, this is likely caused by the increased upstream excitatory activation. These results show that a decrease in DG granule cell number causes increase in the proportion strongly activated in DG by exploration of a novel environment which affects the downstream areas such as CA1, even though CA1 should have been without direct effect from ADX.

If ADX animals had increased locomotion and exploration of an environment then the increase in number of active cells seen in DG CA3 and CA1 could be due to increased use of place cells. The rats would have passed over place cell firing fields more often and would be more likely to cover the entire environment instead of possibly partially exploring. A study completed by Islam et al. (1996) looked at spatial learning and novel open field exploration after ADX. Locomotion and rearing were measured for open field. They reported no difference in amount of locomotion and a deficit in ADX rearing at only one time point showing ADX animals do not have increased exploratory behaviour. To add to this, no study has reported a difference in ADX exploration behaviour during radial arm maze, object context mismatch, or

novel object discrimination. With no report of differences in exploration behaviour in other studies and no difference when specifically tested by Islam et al. we can conclude ADX animals do not have different exploratory behaviour than control and assume exploration of the contexts in experiments preformed was similar in all groups.

The behaviour of granule cell depleted animals has been documented in a wide variety of task and only express a deficit in complex memory tasks (Vaher et al., 1994; Sutherland et al., 1983). The task that appears to be most sensitive to this deficit is object-context mismatch. This task requires a rat to bind in memory a particular object with a specific context (Spanswick et al., 2010). Rats are exposed to two distinctly different environments, each with a pair of identical objects, but a different object pair is located in the two environments. After multiple exposures to these contexts the rat is placed in one of the familiar environments with one of each object pair. Control rats explore the object that is novel to the current environment more than the object that has been shown with the environment previously. ADX rats show no preference for either object. In similar experiments it was shown in a constant familiar single environment ADX rats prefer to explore novel over familiar objects. The deficit in object-context mismatch likely reflects an inability to differentially respond to the two contexts, or a deficit in object-context binding.

The H1a results point to a possible basis for the deficit in this memory tasks and related behavioural tasks. We see at least a 3 fold increase in all 3 hippocampal

subfields in ADX, while incomplete ADX animals show a slight increase in DG and return to control levels in CA1. Perhaps entorhinal cortex and hippocampal circuitry can compensate for any minor disruption seen in incomplete ADX animals DG. We can speculate about what is occurring in hippocampal place fields during this dramatic increase in H1a positive cells in the hippocampus. Normally a specific environment is represented by a reliable firing pattern of a specific subset of hippocampal place cells. If the number of active cells increases dramatically then downstream regions may not be able to generate distinctively different representations of different environments. There are 2 possibilities of how the hippocampus with reduced granule cells is impaired in representing an environment. It could be the increased H1a expression is due to an increased firing rate in place cells and there is no change in place cell number. An increase firing rate could happen in at least two ways, either the place cells are stable and when activated their spiking behaviour has drastically changed or the fields are unstable and there would be spiking behaviour that is not confined to a single location. Both cases require IEG signal to be activity dependant (discussed later) and would increase the firing rate of the place cells and result in an increase IEG expression over the course of exploration of a single environment.

A second explanation of these results is the 3-fold increase in H1a positive cells is due to an increase in the number of place cells being recruited. Under this possibility place cells would be recruited to represent an area but would not maintain their field and replaced by a new cell. The loss could occur during an

environment exposure or between exposures, unfortunately there is no way for us to tell with this current experiment. This explanation would mean place cells are not reliable and would not consistently represent the same area. To understand what is occurring would require further research of single unit recording after ADX.

One study has looked at single unit recording of place cells after granule cell loss (McNaughton et al., 1989) and found some interesting results. After at least 50% loss of granule cells they recorded from cells in CA3 and CA1 and found that field specificity was unaffected but neurons had lost reliability trial to trial and showed increased "burstiness". When taking this into consideration it does not help figure out which explanation could be correct but suggest that possibly a little bit from all explanations is occurring. The increase "burstiness" suggests it is an increase in firing rate and the reduced reliability could provide evidence for either nonspecific place cell firing or new place cell recruitment. To fully understand this another experiment must be performed. Single unit recording after ADX and lap running would be able to determine which case is correct. During lap running the first measure to look at is place cell reliability lap to lap and trial to trial. If place cells stay in the same location an analysis of firing characteristic would need to be completed to see if there is an increase firing rate. If the place cell fields are moving then nonspecific firing would be the logical answer, and if new place cells are recruited then the last explanation is correct. From the information available at this time no concrete conclusion can be made.

A possible explanation of the increase in H1a positive cells in ADX animals is ADX could affect the process of ETC. ADX might cause cells in the hippocampus to overproduce H1a mRNA in response to action potentials and thus cause a greater number of H1a positive cells to be detected in ADX rats. This could occur if one of the hormones produced by the adrenal glands plays a role in modulating the ETC process or if degeneration of the DG is causing the average production of H1a in remaining cells to be increased. The latter possibility could be due to the change in average age of granule cells and younger cells may produce more H1a mRNA. When considering this possibility it is important to note an increase in H1a positive cells was found in CA3 and CA1. This would mean ADX is affecting the ETC process in all areas of the hippocampus. This would be interesting since there has been no evidence that ADX has any effect on any cell type except DG granule cells. There are many possible explanations of how ETC could be effected by ADX and further research would be required to confirm or disprove this possibility, until then it must be considered as a possible explanation of the results.

It has been reported in the literature IEG expression in the DG is different in dorsal and ventral blades; triple the number of IEG foci were found in the dorsal blade (Chawala et al., 2005). If you combine this result with the fact that ADX causes greater degeneration in the dorsal blade of the DG (fig. 2) it would be interesting to see if the preference for IEG foci to appear in dorsal DG was still present after loss of cells in the DG. The entire DG can also be separated into dorsal and ventral fields (different from dorsal and ventral blades) and dorsal-ventral differences are found

all through the hippocampus (Jung et al., 1994; Moser et al. 1993). The recent IEG and environmental exposure studies have all looked at the dorsal blade of the dorsal DG and for this study we looked at the entire DG and could be and explanation why we saw a lower percent of active cells. It could also be why we found no difference between one and five environments, maybe the one versus five differences is only seen in dorsal blade of the dorsal DG.

One shortcoming of this study was the lack of home cage control group. The conclusions of the study would be strengthened if at least a control home cage group and an ADX home cage control group had been included. Without these groups we cannot definitely say that expression of H1a detected was due to exploration. It could be the labeling procedure and detection methods were not sufficient to see H1a being produced due to the environmental exposure experience. If it is true the H1a positive cells are not being driven by exploration, it would still be an interesting result that base line H1a mRNA is increased after ADX and granule cell loss. Including a home cage controls, especially ADX and control home cage, would have made interpreting the results more clear and easier to understand. Without these groups our conclusions about specific exploration activations are obviously weakened.

The experiment completed is a prelude to another set of experiments. Previous studies have shown that ADX induced cell loss can be reversed along with behavioural deficits (Spanswick et al., 2007) but it is unknown whether cell function

is also normalized. Performing a similar experiment including a group with treatments that restore the number of granule cells to normal levels along with single unit recording would provide insight into how the hippocampus responds to DG regeneration. The information gained from this kind of study could have numerous implications and benefits that could help people suffering from diseases involving cell loss or brain damage.

This experiment also gives us insight into how the brain compensates after a slow loss of cells through apoptosis. We see that cell loss may increase the activity of the directly affected and downstream regions, it could cause confusion and less distinct representations. This could exacerbate the problem because it affects downstream areas with incorrect signaling instead of just silence, which might prevent unaffected regions from providing valid compensatory input. Because of the unique slow cell loss, the apoptotic ADX model would be similar to cell loss seen in early stages of Alzheimer's or other dementias. Further study into how the brain compensates for this type of cell loss could provide insights helping people with these diseases.

Degeneration from ADX seem to occur in a binary fashion, either it is present or not. The CORT level does not predict successful degeneration (fig 4 & 5). When we look at all the individual cases (Fig. 2) there is a clear discontinuity in the distribution of granule cell number in ADX animals from successful degeneration to little or no degeneration. ADX rats that have little degeneration are not significantly different

in granule cell number compared to controls. There is a large gap when you compare the incomplete with the lowest number of cells (188928 cells) to the ADX with the highest number of cells (135475 cells). This clear discontinuity in granule cell number is interesting and requires further study to understand why with the same level of CORT degeneration is triggered or not.

After ADX, granule cell death begins within hours and continues until a plateau of neuron loss is reached approximately 8-12 weeks after surgery (Spanswick et al., 2011). We found that only some rats exhibited granule cell loss while others stayed at control levels. This was also noted by Sloviter et al. (1989), who also found no difference in the CORT levels between groups. They concluded that this was due to incomplete removal of adrenal glands and this was enough to prevent the degeneration even though CORT level were still diminished to successful ADX levels. But other groups such as McCormick et al. (1997) found that incomplete animals had higher CORT levels than ADX that was no different from control levels. The phenomenon of binary distribution of degeneration and the confounding CORT levels found in incomplete animals is something that has not been discussed or even noted in the literature and requires further study to understand.

In this experiment H1a was quantified in a binary fashion, either it was present and thus the cell was active or it was not and we assume the cell was silent. Cells have a baseline firing rate and thus any cell could produce some amount of H1a, there is evidence that the firing rate could impact the amount of H1a signal present (Li,

2011). This should be considered when considering these results since the amount of activation could be playing a role instead of number of cells active. But at this time we do not have available a way of quantifying all of the different intensities of H1a foci. It is still not conclusively demonstrated if IEGs should be thought of in a binary fashion or in a continuous scale dependent on the amount of activation.

Some cautionary points are worth noting. The images analyzed were taken on a nanozoomer. Nanozoomer images are very useful but have bleed through, which is when one channel (red green or blue) picks up signal from a different channel so you get incorrect information on each channel. This was taken into consideration when the counting program was written and why a high threshold was used. The image resolution is limited so finding the right parameters to successfully count H1a foci was less than optimal; because of this we only used one optical slice through each section to prevent counting the same foci twice. The quantification program was written specifically for nanozoomer images of these animals and the threshold was set to count as many foci as possible without counting noise. Even with the lowest possible threshold we did not see Homer 1a foci in every section.

From this information it is obvious that nanozoomer combined with automated counting is not the best method to quantify IEG signal, more foci needed to be counted. A higher resolution is required to see more foci, but with a higher resolution the amount of scan time greatly increases. To obtain confocal images for exhaustive automated counting would take well over 1000 hours of scan time and is

not feasible given access to currently available resources. Another option, which many of the recent IEG experiments have taken, is obtaining a couple of confocal images randomly through your region of interest. This method will allow for a reasonable scan time but can potentially result in very biased results. Using a method like this does not allow for sampling sites through the whole structure and the whole structure will not be represented in the results. The density of activation changes through structures and it is required to have sites from all regions of a structure to get an accurate representation and a good estimate.

The best solution would be using high resolution confocal images in an unbiased stereological fashion (like used for NeuN cell number count) to obtain an estimate of number of cells and probability of activation. This could be done with a reasonable amount of scan time and would give an accurate estimate through a method that has been tested in many different fields and has held up as a useful and accurate method. This method would allow for calculation of the standard error of the estimate. This is extremely important in determining if enough markers have been counted to allow for statistical proof that groups are different. It allows for representation of all areas of the structure you are counting so there is no worry for biased counting. Unfortunately we do not have the equipment required to do this at this time.

Even with the short-comings in the technique used we were still able to see a large and significant difference in the activation pattern after loss of granule cells. This speaks to how robust and significant this effect is. Compared to controls, ADX

animals had more Homer 1a positive cells in all subfields (DG, CA3 and CA1). The change in hippocampal activity is congruent with the behavioural data showing deficit in object context mismatch. The results show that after loss of granule cells the perforant path over stimulates the DG cause a large increase in number of active cells that propagates through the entire hippocampus. Most likely individual place cell specificity remains unchanged (McNaughton et al., 1989) so the increase is probably caused by place cell maps not being tied to an environment and switching between multiple maps which produces an increase in activation.

References

Alme CB, Buzzetti RA, Marrone DF, Leutgeb JK, Chawla MK, Schaner MJ, Bohanick JD, Khoboko T, Leutgeb S, Moser EI, Moser MB, McNaughton BL, Barnes CA. (2010) Hippocampal Granule Cells Opt for Early Retirement. *Hippocampus 20*: 1109-1123

Amaral, D.G., Witter, M.P. (1989) The three-dimensional organization of the hippocampal formation: A review of anatomical data. *Neuroscience 31(3)*: *571 – 591*

Armstrong JN, McIntyre DC, Neubort S, Sloviter RS. (1993) Learning and memory after adrenalectomy induced hippocampal dentate granule cell degeneration in the rat. *Hippocampus 3*(3): 359-371

Brakeman PR, Lanahan AA, O'brien R, Roche K, Barnes CA, Huganir RL, Worley PF. (1997) Homer: a protein that selectively binds metabotropic glutamate receptors. *Nature 386*: 284 – 288

Cameron HA, and Gould E. (1996) Distinct Populations of cells in the adult dentate gyrus undergo mitosis or apoptosis in response to adrenalectomy. *The journal of comparative neurology 369*: 56-63

Chadderton P, Margrie TW, Hausser M. (2004) Integration of quanta in cerebellar granule cells during sensory processing. *Nature 428*: 856 – 860

Chawla MK, Guzowski JF, Ramirez-Amaya V, Lipa P, Hoffman KL, Marriott LK, Worley PF, McNaughton BL, Barnes CA. (2005) Sparse, Environmentally selective expression of Arc RNA in the upper blade of the rodent fascia dentate by brief spatial experience. *Hippocampus 15*: 579 – 586

Daumas S, Ceccom J, Halley H, Frances B, Lassalle JM (2009) Activation of metabotropic glutamate receptor type 2/3 supports the involvement of the hippocampal mossy fiber pathway on contextual fear memory consolidation. *Learning and Memory 16*: 504-507

Gould E, Woolley CS, McEwen BS. (1990) Short-term glucocorticoid manipulations affect neuronal morphology and survival in the adult dentate gyrus. *Neuroscience 37*(2): 367 – 375

Hennou S, Kato A, Schneider EM, Lundstrom K, Gahwiler BH, Inokuchi K, Gerber U, Ehrengruber MU. (2003) Homer – 1a/vesl – 1S enhances hippocampal synaptic transmission. *European Journal of Neuroscience 18*: 811 – 819

Jaarsma D, Postema F, Korf J. (2004) Time course and distribution of neuronal degeneration in the dentate gyrus of rat after adrenalectomy: A silver impregnation study. *Hippocampus 2*: 143 – 150

Jung MW, Wiener SI, McNaughton BL. (1994) Comparison of spatial firing characteristics of units in dorsal and ventral hippocampus of the rat. *The Jounral of Neuroscience 14*(12): 7347 - 7356

Kolb B, and Whishaw IQ. (2011) An introduction to Brain and Behaviour (3rd ed.). New York: *Worth Publishers.*

Kim JJ, and Fanselow MS. (1992) Modality – Specific retrograde amnesia of fear. *Science 256*: 675 – 677

Lanahan A, and Worley P. (1998) Immediate – early genes and synaptic function. *Neurobiology of learning and memory 70*: 37 – 43

Leutgeb S, and Leutgeb JK (2007) Pattern separation, pattern completion and new neuronal codes within a continuous CA3 map. *Learning and Memory 14*: 745 – 757

Leutgeb S, Leutgeb, JK, Barnes CA, Moser EI, McNaughton BL, Moser MB. (2005) Independent Codes for Spatial and Episodic Memory in Hippocampal Neuronal Ensembles. *Science 309*: 619 – 623

Li Wing, Use of immediate-early gene activation analyses to compare hippocampal sub region activity during spatial navigation. M.Sc. Thesis, University of Lethbridge: December 2011

McCormick CM, McNamara M, Mukhopadhyay S, Kelsey JE. (1997) Acute corticosterone replacement reinstates performance on spatial and nonspatial memory tasks 3 months after adrenalectomy despite degeneration in the dentate gyrus. *Behavioural Neuroscience 111*(3): 518 – 531

McNaughton BL, Battaglia FP, Jensen O, Moser EI, Moser MB. (2006) Path integration and the neural basis of the 'cognitive map'. *Nature Reviews Neuroscience 7*: 663 – 678

McNaughton BL, Barnes CA, Meltzer J, Sutherland RJ. (1989) Hippocampal granule cells are necessary for normal spatial learning but not for spatial – selective pyramidal cell discharge. *Experimental Brain Research 76*: 485 – 496

Mittelstaedt ML, and Mittelstaedt H. (1980) Homing by path integration in a mammal. *Naturwissenschaften* 67: 566 - 567

Morris RGM, Garrud P, Rawlins JNP, O'Keefe J. (1982) Place navigation impaired in rats with hippocampal lesions. *Nature 297*: 681 – 683

Moser E, Moser MB, Andersen P. (1993) Spatial learning impairment parallels the magnitude of dorsal hippocampal lesions, but is hardly present following ventral lesions. *The Journal of Neuroscience 13*(9): 3916 - 3925

Muller R. (1996) A Quarter of a Century of Place Cells. *Neuron 17*: 979 – 990

Muller RU, and Kubie JL. (1987) The effects of changes in the environment on the spatial firing of hippocampal complex-spike cells. *The Journal of Neuroscience 7*(7) 1951 – 1986

O'Keefe J, and Dostrovsky J. (1971) The hippocampus as a spatial map. Preliminary evidence form unit activity in the freely-moving rat. *Brain Research 34*: 171 – 175

Schmidt-Hieber C, Jonas P, Bischofberger J (2004). Enhanced synaptic plasticity in newly generated granule cells of the adult hippocampus. *Nature 429*: 184 – 187

Scoville WB, and Milner B. (1957) Loss of recent memory after bilateral hippocampal lesions. *J Neurol Neurosurg Psychiatry 20*: 11 – 21

Sloviter RS, Valiquette G, Abrams GM, Ronk EC, Sollas AL, Paul LA, Neubort S. Selective loss of hippocampal granule cells in the mature rat brain after adrenalectomy. *Science 243*: 535 – 538

Sousa N, Madeira MD, Barbosa PMM. (1997) Structural alteration of the hippocampal formation of adrenalectomized rats: an unbiased stereological study. *Journal of Neurocytology 26*: 423 – 438

Spanswick SC, Lehmann H, Sutherland RJ. (2011) A novel animal model of hippocampal cognitive deficits, slow neurodegeneration, and neuroregeneration. *Journal of Biomedicine and Biotechnology 2011*

Spanswick SC, and Sutherland RJ. (2010) Object/context-specific memory deficits associated with loss of hippocampal granule cells after adrenalectomy in rats. *Learning and Memory 17*: 241 – 245

Spanswick SC, Epp JR, Keith JR, Sutherland RJ. (2007) Adrenalectomy-Induced granule cell degeneration in the hippocampus causes spatial memory deficits that are not reversed by chronic treament with corticosterone or fluoxetine. *Hippocampus 17*: 137 – 146

Sutherland RJ, and McDonald RJ. (1990) Hippocampus, amygdala and memory deficits in rats. *Behavioural Brain Research 37*: 57-79

Sutherland RJ, Whishaw IQ, Kolb B. (1982) A behavioural analysis of spatial localization following electrolytic, kainite or colchicine-induced damage to the hippocampal formation in the rat. *Behavioural Brain Research 7*: 133 – 153

Sutherland RJ, O'Brien J, Lehmann H. (2008) Absence of systems consolidation of fear memories after dorsal, ventral or complete hippocampal damage. *Hippocampus 18*(7): 710 - 718

Sutherland RJ, and Lehmann H. (2011) Alternative conceptions of memory consolidation and the role of the hippocampus at the systems level in rodents. *Current Opinion in Neurobiology 21*: 446 – 451

Treves A, and Rolls ET. (1992) Computational constraints suggest the need for two distinct input systems to the hippocampal CA3 network. *Hippocampus 2*: 189 – 200

Vaher PR, Luine VN, Gould E, McEwen BS. (1994) Effects of adrenalectomy on spatial memory performance and dentate gyrus morphology. *Brain Research 656*: 71 – 78

Woolley CS, Gould E, Sakai RR, Spencer RL, McEwen BS. (1991) Effects of aldosterone or RU28362 treatment on adrenalectomy-induced cell death in the dentate gyrus of the adult rat. *Brain Research 554*(1-2): 312 – 315

Xavier GF, Oliveira-Filho JB, Santos AMG. (1999) Dentate gyrus-selective colchicine lesion and disruption of performance in spatial tasks: Difficulties in "place strategy" because of a lack of flexibility in the use of environment cues?. *Hippocampus 9*: 668 – 681

Xiao B, Tu JC, Worley PF. (2000) Homer: a link between neural activity and glutamate receptor function. *Current Opinion in Neurobiology 10*: 370 – 374

Zhongting H, Kazunari Y, Hitoshi O, Haiping L, Mitsuhiro K. (1997) The *in vivo* time course for elimination of adrenalectomy – induced apoptotic profiles from the granule cell layer of the rat hippocampus. *The Journal of Neuroscience 17(*11): 3981 - 3989

Appendix 1

One vs Five Environments

When originally designing the experiment we planned to see how ADX and control animals activation pattern differed. After obtaining our results we found that control rats showed no difference in number of H1a positive cells after exposure to 1 vs 5 environments. In the DG of control rats mean number of homer foci per slide for one environment was 0.0593 ± 0.0092 and five environments was 0.0579 ± 0.0287 and showed no statistical difference ($p = 1.000$). In CA3 control rats exposed to one environment mean foci number was 1.170 ± 0.228 and exposure to five environments was 1.131 ± 0.610, once again there was no statistical difference ($p = 1.000$). Finally in CA1 one environment mean foci was 2.235 ± 0.961 and five

environments was 2.057 ± 1.138 p = 1.000. Since there was no statistical difference between control groups therefore we collapsed 1 and 5 environment groups in all subsequent analyses.

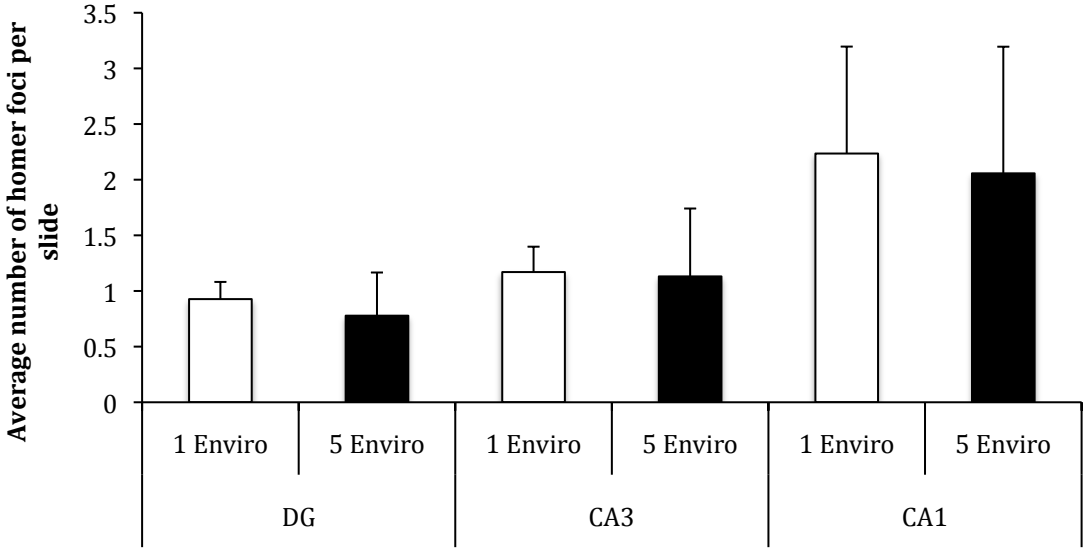

Figure 12: Mean Number of homer 1a positive neurons in each of the hippocampal subfields for control animals. There is no difference between exposure to 1 environment or 5 environments in any hippocampal area. We collapsed these groups because of this data.

Appendix 2

Automated H1a counting program

This is an automated counting program designed to count H1a foci labeled with a FITC fluorescent probe and imaged on nanozoomer. Due to the nature of FISH labeling and nanozoomer imaging exact parameters used for this analysis are designed for the images used and different parameters may be required for other

FISH batches and experiments. This program sets a minimum value for green channel and sets the rest of the green channel too zero this function as the minimum parameter. A ratio of green and blue channel value is used to account for any bleed through and then it scans through the green pixels to find a maximum. Once list of maxima are found subsequent exclusion measure are take to ensure the foci is in fact a H1a positive cell such as, in a DAPI cell, not close to a second foci, and correct size. The program was coded using Matlab and requires images to be in .bmp format.

```
%cd('/users/ep1205/Documents/MATLAB/James/Images')
cd('E:\Matt\DG-Converted')
%cd('C:\users\james.cardiff\Desktop\Image')
%cd('C:\Users\james.cardiff\Documents\MATLAB\Images')
filelist = dir; %comand to make matrix of strings for file names
BlobMatrix = [];

time = [];

u = 3;
for u = 3:length(filelist)
percentdone = u/length(filelist)*100
tic;
imagefile = filelist(u);

IT = imread(imagefile.name);
% IT = IT(350:500,680:800,:);
% IT = IT(160:180,50:65,:);
green = IT(:,:,2);
blue = IT(:,:,3);
composite = IT;
%green = IT(450:550,300:400,2);
%composite = IT(450:550,300:400,1:3);
ix = 1;
iy = 1;
s = size(green);
minimum = 9;  %%%%%%%%%%%%%%%%%%%%%%%%%%%
f = zeros(s);
ratio = 3.5;

[x y] = find(green > minimum);
greenpix = length(x);

%%
%CONVOLUTION
%finds the green pixels then averages the pixel based off
%of surrounding pixels green value
```

```
for i = 1:greenpix
    ix = x(i);
    iy = y(i);

    %sets up a square with high (h) and low (l) for x and y

    hx = ix+2;
    lx = ix-2;
    hy = iy+2;
    ly = iy-2;

    %if statements for edges of box to analyze

    if hx > length(green(:,1))
        hx = length(green(:,1));
    end
    if hy > length(green(1,:))
        hy = length(green(1,:));
    end
    if lx < 1
        lx = 1;
    end
    if ly < 1
        ly = 1;
    end

    %this calculates the average
   f(ix,iy) = mean(mean(green(lx:hx,ly:hy)));
end

% Takes ratio of blue to green and if the green isn't high enough sets
% the green channel to zero

f = f.*10;
composite(:,:,2) = f;
for i = 1:greenpix
    if blue(x(i),y(i))/ green(x(i),y(i)) > ratio
        f(x(i),y(i)) = 0;
    end
end

green = f;
composite(:,:,2) = green;

k = f;
%%
%%STEP ONE IN FINDING MAXIMA
%sets pixel to zero if there is a pixel within a 7x7
%block surounding it
%this allows each blob to be converted into one point


for i = 1:length(x)

    %same high low x y fomula used here with if statements to control
the
```

```
    %edges

    hx = x(i)+5;
    lx = x(i)-5;
    hy = y(i)+5;
    ly = y(i)-5;

    if  hx > length(green(:,1))
        hx = length(green(:,1));
    end
    if hy > length(green(1,:))
        hy = length(green(1,:));
    end
    if lx < 1
        lx = 1;
    end
    if ly < 1
        ly = 1;
    end

    B = find(k(lx:hx,ly:hy));

    if length(B) > 1 == 1
        k(x(i),y(i)) = 0;
    end
end

%%
%FINDS MAXIMA
%finding maxima location to be counted
%takes info from previous loop and finds maxima
%that is within 8x8 block around the point
%[Q W] is matrix of maxima locations

[x y] = find(k > 0);
Q = zeros(length(x),1);
W = zeros(length(x),1);
e=1;

for i = 1:length(x)

    if x(i) > length(green(:,1))-2 == 1
        x(i) = length(green(:,1))-2;
    end
    if x(i) < 7
        x(i) = 7;
    end
    if y(i) > length(green(1,:))-3 == 1
        y(i) = length(green(1,:))-3;
    end
    if y(i) < 6
        y(i) = 6;
    end

    rowStart = x(i)-6;
    colStart = y(i)-5;
```

```
    o = f(x(i)-6:x(i)+1,y(i)-5:y(i)+2);
    [value L] = max(o(:));
    [q w] = ind2sub(size(o),L);
    % move indexes to correct spot in matrix
    q = q + rowStart-1;
    w = w + colStart-1;
    Q(e) = q;
    W(e) = w;
    e = e+1;

end

%%
%SIZE MINIMUM
%eliminates small blobs
%[O P] is the maxima quardinates with size minimum

minsize = 8; %%%%%%%%%%%%%%%%%%%%%%%%%%%%%%%%%%
m = zeros(7,7);
n = 1;
O = [];
P = [];
i = 1;
e = 1;
exclusionSIZE = [];  % this gives quardinates of excluded blobs
for i = 1:length(Q)
   m = f(Q(i)-3:Q(i)+3,W(i)-3:W(i)+3);
   blobsize = find(m);
   blobsize = length(blobsize);
   if blobsize > minsize == 1
       O(n,1) = Q(i);
       P(n,1) = W(i);
       n = n+1;
   end
   if blobsize <= minsize == 1
       exclusionSIZE(e,:) = [Q(i) W(i)];
       e = e+1;
   end

end

%%
%BLOB in DAPI
%finds number of blue pixels around blob

minbluepix = 15; %%%%%%%%%%%%%%%%%%%%%%%%%
blueintensity = 30;
n = 1;
G = [];
H = [];
e = 1;
exclusionBLUE = [];  %quardinates of blobs excluded because of lack of
blue
for i = 1:length(O)

    hx = O(i)+25;
    lx = O(i)-25;
```

```
    hy = P(i)+25;
    ly = P(i)-25;

    if  hx > length(green(:,1))
        hx = length(green(:,1));
    end
    if hy > length(green(1,:))
        hy = length(green(1,:));
    end
    if lx < 1
        lx = 1;
    end
    if ly < 1
        ly = 1;
    end

    DAPIcheck = blue(lx:hx,ly:hy);
    DAPIcheck = find(DAPIcheck>blueintensity);

    if length(DAPIcheck) > minbluepix == 1
        G(n,1) = O(i);
        H(n,1) = P(i);
        n = n+1;
    end
    if length(DAPIcheck) <= minbluepix == 1
       exclusionBLUE(e,:) = [O(i) P(i)];
       e = e+1;
   end
end
```

```
%%
%FINDS DISTANCE BETWEEN MAXIMA
%uses d = formula to find distance in pixels
%creates matrix D with all the distances between
%all the different maxima


D = zeros(length(G),length(H));
for i = 1:length(G)
    for j = 1:length(H)
    d = sqrt((G(i)-G(j)).^2+(H(i)-H(j)).^2);
    D(i,j) = d;
    end
end

%%
%ELIMNATES MAXIMA
%if 2 maxima are close only counts them as one (by subtracting half)

% D1 = D;
% Double = 0;
% Distance = 30;  %%%%%%%%%%%%%%%%%%%%%%%%%%%%%%%%
```

```
% for i = 1:length(D)
%     for j = 1:length(D)
%         if D(i,j) <= Distance == 1 && D(i,j)>1 == 1
%             D1(i,j) = 0;
%             Double = Double+0.5;
%         end
%     end
% end

%%
%Identifies counted blobs
%  distance rejects are still shown


% figure;
% image(composite)
% hold on
% scatter(H,G,24,[1 0 0])
% numBlobs = length(D);%-Double; %%%%%%%%%%%%%%%%%%%%%%%%%%


% if strfind(imagefile.name,'DG') > 0
%     BlobMatrix(u,1) = numBlobs;
% end
%
% if strfind(imagefile.name,'CA3') > 0
%     BlobMatrix(u,2) = numBlobs;
% end
%
% if strfind(imagefile.name,'CA1') > 0
%     BlobMatrix(u,3) = numBlobs;
% end

%%
ratstring = strfind(imagefile.name,'-');
rat = imagefile.name(ratstring(end)+1:ratstring(end)+2);
rat = str2double(rat);
if rat <= 49 == 1
    rat =
str2double(imagefile.name(ratstring(end)+2:ratstring(end)+3));
end



slidestring = strfind(imagefile.name,'Slide');
slidestring = imagefile.name(slidestring+5:slidestring+7);
slide = str2double(slidestring);
if isnan(slide) == 1
    slide = str2double(slidestring(1));
end


% Still need to find way to tell difference between region
% images have section number at the end so it will be difficult
% to tell them apart by last digit
```

```
% if strfind(imagefile.name,'DG') > 0
%     region = 0;
% end
% if strfind(imagefile.name,'CA1') > 0
%     region = 1;
% end
% if strfind(imagefile.name,'CA3') > 0
%     region = 2;
% end
%
region = 0;

if strcmp(imagefile.name((end)-6),'_') == 1;
    region = 0;
end
if strcmp(imagefile.name((end)-6),'1') == 1;
    region = 1;
end
if strcmp(imagefile.name((end)-6),'2') == 1;
   region = 2;
end

numBlobs = length(D);



%BlobMatrix = [Rat# Slide# #ofBlobs Region]
                                % 0=DG 1=CA3 2=CA1
BlobMatrix(u-2,1) = rat;
BlobMatrix(u-2,2) = slide;
BlobMatrix(u-2,3) = numBlobs;
BlobMatrix(u-2,4) = region;


time(u,1) = toc;
end

save('BlobMatrixDG.mat', 'BlobMatrix')
```

Stereology estimate program

This program was used to mimic the optical fractionator technique used by microbrightfield. This was written to obtain cell estimates same images used to

obtain H1a foci counts. The same images were used so we could get an accurate number for percent active instead of using an ambiguous number of activity if NeuN counts were used.

```
function varargout = Stere(varargin)
% STERE MATLAB code for Stere.fig
%      STERE, by itself, creates a new STERE or raises the existing
%      singleton*.
%
%      H = STERE returns the handle to a new STERE or the handle to
%      the existing singleton*.
%
%      STERE('CALLBACK',hObject,eventData,handles,...) calls the local
%      function named CALLBACK in STERE.M with the given input
arguments.
%
%      STERE('Property','Value',...) creates a new STERE or raises the
%      existing singleton*.  Starting from the left, property value
pairs are
%      applied to the GUI before Stere_OpeningFcn gets called.  An
%      unrecognized property name or invalid value makes property
application
%      stop.  All inputs are passed to Stere_OpeningFcn via varargin.
%
%      *See GUI Options on GUIDE's Tools menu.  Choose "GUI allows only
one
%      instance to run (singleton)".
%
% See also: GUIDE, GUIDATA, GUIHANDLES

% Edit the above text to modify the response to help Stere

% Last Modified by GUIDE v2.5 18-Oct-2012 10:52:29

% Begin initialization code - DO NOT EDIT
gui_Singleton = 1;
gui_State = struct('gui_Name',       mfilename, ...
                   'gui_Singleton',  gui_Singleton, ...
                   'gui_OpeningFcn', @Stere_OpeningFcn, ...
                   'gui_OutputFcn',  @Stere_OutputFcn, ...
                   'gui_LayoutFcn',  [] , ...
                   'gui_Callback',   []);
if nargin && ischar(varargin{1})
    gui_State.gui_Callback = str2func(varargin{1});
end

if nargout
    [varargout{1:nargout}] = gui_mainfcn(gui_State, varargin{:});
else
    gui_mainfcn(gui_State, varargin{:});
end
% End initialization code - DO NOT EDIT
```

```
% --- Executes just before Stere is made visible.
function Stere_OpeningFcn(hObject, eventdata, handles, varargin)
% This function has no output args, see OutputFcn.
% hObject    handle to figure
% eventdata  reserved - to be defined in a future version of MATLAB
% handles    structure with handles and user data (see GUIDATA)
% varargin   command line arguments to Stere (see VARARGIN)

% Choose default command line output for Stere
handles.output = hObject;
global countingframe countingratio Q W results c imagenumber
imagenumber = 0;
results = 0;
Q = [];
W = [];
c = 0;
countingframe = 100;%%%%%%%%%%%%%%%%%%
countingratio = 5;%%%%%%%%%%%%%%%%%%%%
% Update handles structure
guidata(hObject, handles);

% UIWAIT makes Stere wait for user response (see UIRESUME)
% uiwait(handles.figure1);


% --- Outputs from this function are returned to the command line.
function varargout = Stere_OutputFcn(hObject, eventdata, handles)
% varargout  cell array for returning output args (see VARARGOUT);
% hObject    handle to figure
% eventdata  reserved - to be defined in a future version of MATLAB
% handles    structure with handles and user data (see GUIDATA)

% Get default command line output from handles structure
varargout{1} = handles.output;


% --------------------------------------------------------------------
function Count_OnCallback(hObject, eventdata, handles)
% hObject    handle to Count (see GCBO)
% eventdata  reserved - to be defined in a future version of MATLAB
% handles    structure with handles and user data (see GUIDATA)

global Q W c
[q w] = ginput;
plot(q,w,'.y')
Q(c+1:c+length(q),1) = q;
W(c+1:c+length(w),1) = w;
c = c+length(w);

% --------------------------------------------------------------------
function Sum_ClickedCallback(hObject, eventdata, handles)
% hObject    handle to Sum (see GCBO)
% eventdata  reserved - to be defined in a future version of MATLAB
% handles    structure with handles and user data (see GUIDATA)
```

```
cd('/Users/ep1205/Documents/MATLAB/James')
global Q W countingratio sum results imagenumber
sum = length(Q)*countingratio^2;
results(imagenumber,1) = sum;

Q = [];
W = [];


% --------------------------------------------------------------------
function Next_ClickedCallback(hObject, eventdata, handles)
% hObject    handle to Next (see GCBO)
% eventdata  reserved - to be defined in a future version of MATLAB
% handles    structure with handles and user data (see GUIDATA)

global imagenumber countingratio countingframe

cd('/Users/ep1205/Desktop/James/Stereology program images/Rat 73')
filelist = dir;
imagefile = filelist(imagenumber+4).name;
p = imread(imagefile);

cd('/Users/ep1205/Documents/MATLAB/James')

% p = imread('Block3-Slide18 -85a_DG_4.png');
% image(p)
% x = p(5250:5750,250:750,:);

display = p;
s = size(display);
i = 1;
countingframe = 100; %%%%%%%%%%%%
countingratio = 5; %%%%%%%%%%%%

startx = randi(countingframe);
starty = randi(countingframe);
x = floor((s(2)-startx)/(countingframe*countingratio));
y = floor((s(1)-starty)/(countingframe*countingratio));


gridx = zeros(1,x);
gridy = zeros(1,y);

for i = 0:x
    gridx(i+1) = startx+((countingframe*countingratio)*i);
end

for i = 0:y
    gridy(i+1) = starty+((countingframe*countingratio)*i);
end

grid = zeros(length(gridx),length(gridy),2);
for i = 1:length(gridx)
    for j = 1:length(gridy)
        grid(i,j,1) = gridx(i);
```

```
        grid(i,j,2) = gridy(j);
    end
end

Gx = gridx;
Gy = gridy;


blueminintensity = 40; %%%%%%%%%%%%%%%%%%
blueminnumber = 250;  %%%%%%%%%%%%%%%%%%
x = [];
y = [];
k = 1;

%Detects amount of blue in counting frame and eliminates frames without
%enough blue

for i = 1:length(gridy)-1
    for j = 1:length(gridx)-1
        n = display(gridy(i):gridy(i)+100,gridx(j):gridx(j)+100,3);
        n = find(n>blueminintensity);
    if length(n)>blueminnumber == 1
        x(k,1) = gridx(j);
        y(k,1) = gridy(i);
        k = k+1;
    end
    end
end

gridx = x;
gridy = y;



%Makes the counting frames
i = 1;
j = 1;
for i = 1:length(gridy)
display(gridy(i):gridy(i)+countingframe,gridx(i),1) = 255;
display(gridy(i):gridy(i)+countingframe,gridx(i)+countingframe,2) =
255;
display(gridy(i),gridx(i):gridx(i)+countingframe,1) = 255;
display(gridy(i)+countingframe,gridx(i):gridx(i)+countingframe,2) =
255;
end

hold on
cla
image(display)
plot(grid(:,:,1),grid(:,:,2),'r+')

imagenumber = imagenumber+1;
```

Appendix 4

H1a Probe Sequence

The H1a probe is obtained in a plasmid and is flanked on either side by RNA polymerase promoter elements. The sequence of the antisense strand is given bellow with the section homologous to the homer protein shown in green.

(SENSE)GGGGGACCTCACGCGGTGGCGGCCGCTCTAGAACTAGTGGATCCCCCGGGCTGC
AGG(EcoRI)AATTCGCGGCCGCCTCAAAGGCAATAATAAATAGCACCATCA
CTCCAAACATGACATTTACTAAAACATCTCAAAAGTTTGGCCAATGGGCTGATAGCCGGG
CAAACACTGTTTATGGACTGGGATTCTCCTCTGAGCATCATCTCTCAAAATTT
GCAGAAAAGTTTCAGGAATTTAAAGAAGCTGCTCGGCTGGCAAAGGAGAAGTCGCAGGA
GAAGATGGAACTGACCAGTACCCCTTCACAGGAATCAGCAGGAGGAGATCTTCA
GTCTCCTTTAACACCAGAAAGTATCAATGGGACAGATGATGAGAGAACACCCGATGTGA
CACAGAACTCAGAGCCAAGGGCTGAGCCAGCTCAGAATGCATTGCCATTTTCAC
ATAGGTACACATTCAATTCAGCAATCATGATTAAATGAGATGGATAAATATGAAGTTCA
TTTGGTTTCAGAAACTCTTGAGTGAAAAATCCCAGGTCAGACTTCTTTAATTAA
TTAATTGTTTGCTGTTGCTCAGATTGACTGAATATTTCCATTATCTGTGTAGAAAAAGG
AACGTTAATTATAGGAGAAACTTTTTCAATGGACAAAACATTCCATTCTATCTA
TATTTTAAAGATCCCTTTTGCTAACCAGTTTTCTGATTTTCTACATGTTACGTAAGACTA
ATAACTTGTGATTAGGATCAATGGACTCCTGCTCCAAAGGAAAGCCTTGCCAC
AGGCCCACAGAGGTGCCACAGAGGACGGGGCCAGGCAGGAACCCGTCAGCATTGAAGGTT
GTTTTTGTATGCCAACAGGAGGAAAGCTTGAGTTGCTGCTGATTCTTAAAAGA
ATTCTGTATTCTAAAAGATACACATCATGTTCTAAATGCATTTTAAACTAGTGACATTA
GTTATTGGCATACTGTGTATTACTAGACTACAAAGAGGATATGAGTGCACCATT
GAAAGTATTTTTTTTAAAAGCCTGTCTACCTTAACACTAATTTTTACCCTTATTTAAATG
CTTTTTACTAAACAGTTTAGTTAAATTAAGAAAACAGTTTGTGACTGCACATC
TTTAGAGAACACCTTTTAAAGAATACATTCTTGACGGATAATGCCAAGTGAGAATATTC
AATCTACTGATTATGCGTGAACTGCATTATACGGACTACGGATTAACCTTAGCT